TRISAT-R: FLIGHT EXPERIENCE IN MEO

Lorenzo Gonzales [(1)], Kenza Benamar [(2)], Giovanni Santin [(3)], Salvatore Danzeca [(4)], Iztok Kramberger [(1)]

[(1)] *Faculty of Electrical Engineering and Computer Science, University of Maribor, Koroška cesta 46, 2000 Maribor, Slovenia, lorenzo.gonzales@um.si*
[(2)] Technology Program Office (GSTP), *European Space Agency (ESA), 2200 AG, Noordwijk, The Netherlands, kenza.benamar@esa.int*
[(3)] *Directorate of Technology, Engineering and Quality (D/TEC), European Space Agency (ESA), 2200 AG, Noordwijk, The Netherland, giovanni.santin@esa.int*
[(4)] *Section Leader BE-CEM-EPR, CERN, Esplanade des Particules 1, 1211 Geneva 23, Switzerland, salvatore.danzeca@cern.ch*

ABSTRACT

This paper highlights the technical achievements and presents the in-flight experience of one of the first successful 3U nanosatellite mission in medium earth orbit (MEO) in Europe, TRISAT-R. TRISAT-R is an institutional non-commercial nanosatellite mission primed by the University of Maribor under the contract with ESA and in cooperation with CERN and Slovenian company SkyLabs. The primary mission objective is measurement of ionizing radiation and characterization of the space environment, consolidating the environmental models by comparing the simulated high energy particles particle environment with the measured data in orbit. The radiation measurements are conducted with several scientific payloads to monitor the Single Event Effects and Total Ionizing Dose. The secondary mission objectives are several In-Orbit demonstrations to show new solutions for nanosatellite component miniaturization, testing new design concepts, and demonstrating new Radiation Hardened by Design mitigation techniques for protection of high-performance and high-density electronic components, and targeting the upcoming era of Artificial Intelligence in space applications. Additionally, the satellite was equipped with two highly miniaturized experimental COTS cameras capturing the black Sun effect, which is a consequence of pixel spillover due to Sun's energy saturation. These cameras captured a view of the Earth from MEO orbit by the 3U nanosatellite.

1 INTRODUCTION

Interest in nanosatellites is continuously growing in the recent year with announced launches surpassing the predicted values by almost 50% [1]. Although nanosatellite missions are subjected to delays as any other space missions, since 2021 we achieve a record high number of launches each year [2]. Furthermore, the nanosatellite trend is shifting from primarily academic missions towards highly sophisticated scientific missions, which are even employed in challenging interplanetary scenarios [3]. It must be noted that most mission using nanosatellites beyond Low Earth orbit (LEO) are a secondary payload of motherships and do not need to employ long range communications towards Earth. Another emerging field targeted by nanosatellites are space probes, which enable multipoint remote sensing applications, where spatial variations need to be measured concurrently [4]. Furthermore, such probes are leaning towards self-sufficiency in terms of power generation, communication with Earth and housekeeping activities to increase their practicality [5]. This trend is developing similarly as the terrestrial Internet of Things (IoT) segment developed, where highly integrated energy efficient electronic devices are utilised for remote sensing [6]. However most of the proposed Internet of Space Assets (IoSA) concepts propose utilisation of Inter Satellite Link (ISL) with mesh network topologies [7], [8], which are due to multiple hops reducing the energy efficiency

of the system. A better approach is the usage of relays that would have reduce the needed communications module output power to transmit the acquired data towards Earth, but currently there are not enough getaways available and usually the gateways are built for specific applications. If we follow the trend of IoT, single-level communication systems are a better approach, but require highly efficient communication modules. Following the later topology, TRISAT-R is a 3U In-orbit demonstration (IOD) mission built as a self-sufficient, highly energy efficient remote sensing probe. TRISAT-R was launched in July 2022 as a secondary payload on the VEGA-C maiden flight along with 5 other nanosatellites varying in size from 1U to 3U. The satellites were deployed in a 70° inclined orbit with an altitude of approximately 6000 km. The target orbit put the satellite in a radiation harsh environment in the inner Van Allen radiation belt, which is another challenge when building highly miniaturised probes, as the volumetric space for shielding is limited. According to [2], in 2024 TRISAT-R is, next to GreenCube, the only operational nanosatellite from the mission and has currently been successfully operational for 21 months (April, 2024).

2 MISSION OVERVIEW

The satellite was deployed in a high radiation environment in Medium Earth Orbit (MEO), where the main radiation sources are electrons and protons trapped by the Earth's magnetic field. The destinated orbit in the inner electron and proton belt can be seen on Figure 1 according to charged particle flux models. The initial radiation simulations were done with SHIELDOSE-2 in SPENVIS [9]. The worst-case radiation model is centre of Aluminium sphere, which in a configuration with minimal (0.05 mm) shielding showed a total ionizing dose (TID) of 177 Mrad per year while the finite Aluminium slab configuration predicted 33 Mrad. The TID inside a 3D body of the satellite with the same shielding is expected to be in-between the predictions for these two shielding configurations. To overcome the predicted extreme TID values, as much shielding as possible was needed, while still satisfying the CubeSat form factor. Accordingly, a 7 mm Aluminium shield was designed around the 3U structure to protect the avionics from effects of ionizing radiation, while still enabling us to fit the solar panels and PC-104 form factor subsystems inside the structure. This led to a 5 kg 3U satellite, of which 3 kg are amounted by structure. The shield with integrated solar panels can be seen on Figure 2. Due to the shield thickness, there was no additional space for deployable panels, which forced us to make the system highly energy efficient.

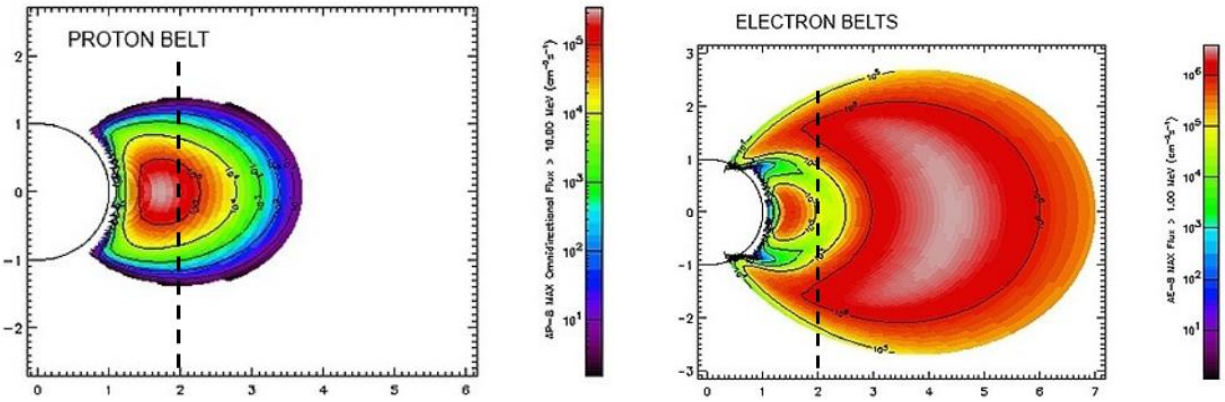

Figure 1. Invariant map of the AP-8 MAX (left) proton integral flux and AE-8 MAX (right) integral flux [9] with marked TRISAT-R orbit.

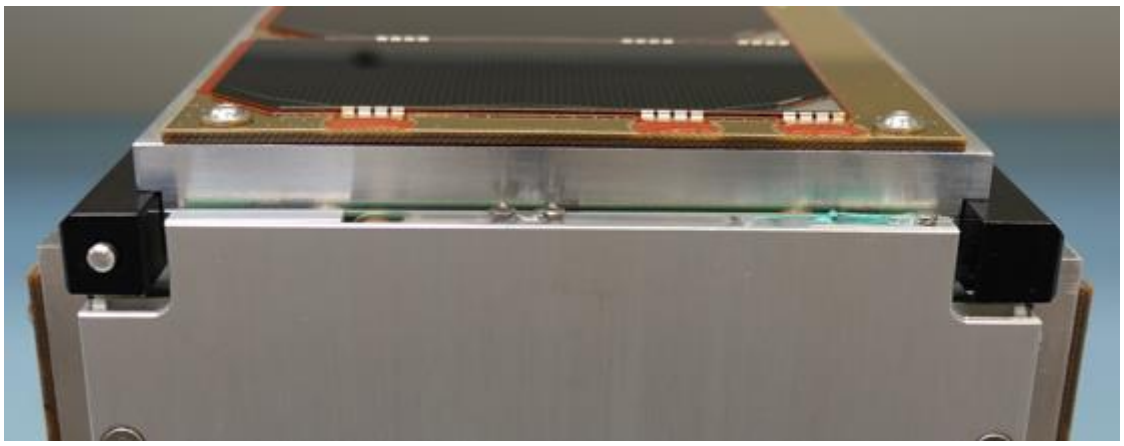

Figure 2. TRISAT-R PFM with visible shield plates and mounted solar panels.

2.1 Mission platform

The TRISAR-R satellite is derived from the TRISAT nanosatellite platform optimized for low power operation in MEO. Due to the limited power production, the nominal operation avionics of the satellite are optimized for low power consumption, especially the Attitude determination and control system (ADCS) and communication systems (COMM). The inner satellites structure with the integrated subsystems is presented in Figure 3. For the power distribution, a highly robust Electronic Power System (EPS) with flight heritage from the TRISAT mission was used. The EPS utilises three LiFePO4 batteries connected in series, with a capacity of 30 Wh, with integrated battery heaters, balancer circuit and a 4 channel analog maximal power tracking [10]. The power is distributed from the EPS with system level current limiters [11], which are enabled according to satellite operation mode. On initial deployment or after a system reset, the satellite is in Safe mode, where only basic avionics are operating (EPS, COMM and ADCS). The satellite is then transitioned by operators to Idle mode, in which the on-board computer (OBC) with primary experiments is enabled. For the secondary experiments, additional high- power modes are available. For ADCS a magnetorquer only mission-purpose system was build.

The ADCS is powered by an 8/16-bit PicoSkyFT processor with floating-point unit and runs a 100 ms regulation loop. The system supports, next to manual mode, three modes of operation: B-dot mode, gyroscope stabilized mode, and sun tracking mode. The gyroscope stabilized mode is a variation of B-dot, but the satellite is not fixed to the magnetic field, but to the angular velocity. The sun tracking mode enables coarse sun tracking with up to 20° of pointing error, but still drastically increases the power production, as the pointing error results in less than 10% power decrease. The ADCS has a power consumption of only 1 W including the magnetorquer consumption, which is very low for actuation in MEO orbit, where the strength of magnetic field is low in comparison to LEO.

The COMM also has a flight heritage from the TRISAT mission, where it proved as a reliable TM/TC module with two redundant TRX chains. The configuration of the module was adjusted to meet the path loss requirements from MEO orbit, which resulted in 163 dB. As the COMM radio output power is only 1.5 W (32dBm), SkyLabs had to build one of the biggest private UHF/VHF ground stations (GS) in Europe to achieve the needed receive signal strength from MEO. The Ground Segment facilitates a UHV receiver antenna configured in 2x2 phase array with 7m Yagi antennas, resulting in 24 dB gain with 10° main lobe. The transmitter antenna is a VHF 2x2 phase array antenna with 20° main lobe and a 1kW power amplifier.

The OBC is designed to facilitate primary radiation experiments via PC-104 interface and periodically logs the experiment data for readout on GS pass.

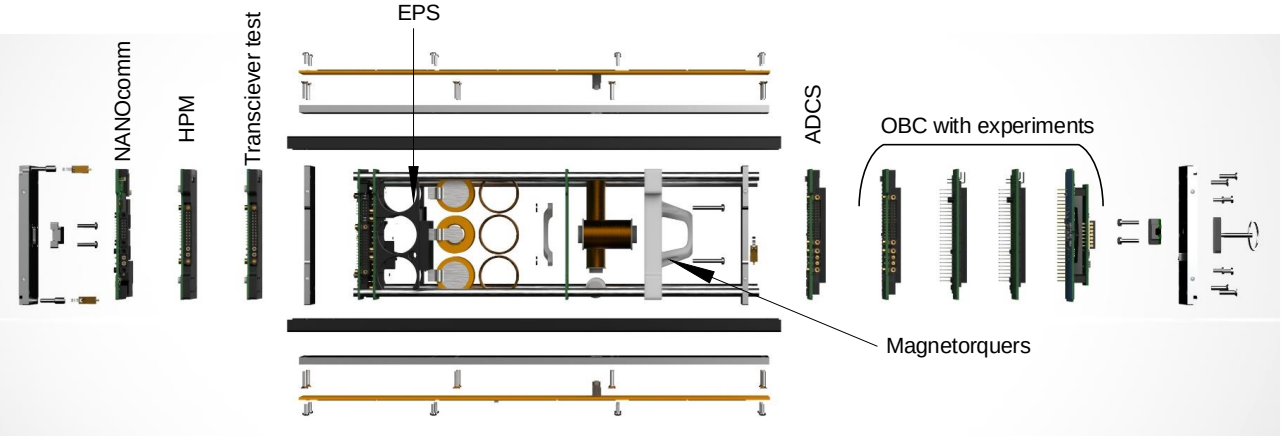

Figure 3. Decomposed TRISAT-R assembly with subsystems

2.2 Scientific payloads

The primary radiation scientific payloads consist of "TID monitor" produced by SkyLabs [12], "CHIMERA" developed by ESA [13], a Floating gate dosimeter ("FGDOS") from iC Malaga [14] and "SpaceRadMon" from CERN [15].

The TID monitor is an encapsulated PIN-diode based sensor, measuring TID per integration cycle of 1.67s. The measurement is thermally compensated and accumulated by the OBC. The TID is logged using a 15-minute interval.

CHIMERA is an in-space testbed for commercial off the shelf (COTS) memories. The experiment monitors single event effects in the memories (SEE), the telemetry readouts report number of single event upsets (SEUs), single event functional interrupts (SEFIs) and possible latch-ups. The experiment is optimized for low power, and it only consumes 62 mW when operational.

The FGDOS is a floating gate (FG) MOSFET sensor, which measures the TID with the reduction of charge in the FG due to ionizing radiation. The sensor enables passive measurement, only the FG charge injection for the FG recharge needs power. The integrated circuit houses two dies of this sensor with digital readout.

SpaceRadMon is a successor from the CELESTA [16] radiation monitor, measuring TID with radiation field effect transistor (RADFET), and SEL and SEU with characterised SRAMs. The TID measurement is passive and absolute, in comparison with FGDOS where the measurement can be passive but requires active recharge cycles.

The radiation experiments are logged with a default logging period of 5 minutes, but the period can be dynamically adjusted.

Additionally, the OBC host two highly miniaturised cameras, which were mounted next to the Sun sensors along the Z axis, as can be seen on Figure 4. The primary goal of the miniaturised cameras is an IOD capturing the black Sun effects, caused by electron spillover on a oversaturated photodiode of the CMOS camera [17]. The integrated cameras have a resolution of 320x320 pixels with Bayer pattern and a 120° field of view.

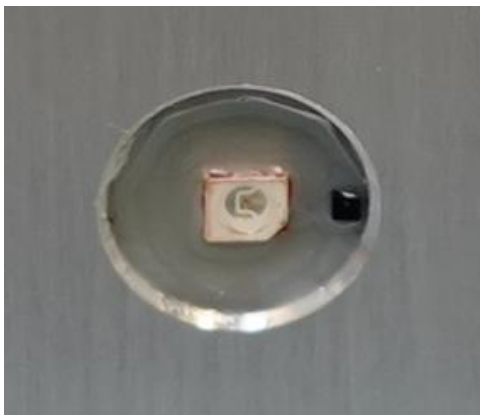

Figure 4. Highly miniaturised camera mounted next to photodiode sun sensor on Z+ plane.

2.3 In-orbit demonstration payloads

Next to primary scientific payloads, two IOD payloads from company SkyLabs are onboard TRISAT-R. First is a transceiver testbed implemented with SkyLabs's NANOLinkv2 designed to verify the operation of S-BAND software defined radio (SDR) chain in a radiation harsh environment. The testbed does not use external antennas, but a simple TX-RX loopback, where PRNG pattern is continuously tested. Up to this date, the test runs in nominal condition, confirming the Radiation Hardened design developed by SkyLabs.

The second IOD payload was the NANOhpm-obc subsystem from SkyLabs, which is a high-performance microcontroller based on Gaisler NOEL-V softcore processor, which is supervised by PicoSkyFT processor. To our knowledge, this was the first RISC-V processor operation in space and most certainly the first RISC-V processor deployed to MEO orbit. The subsystem was utilising artificial intelligence (AI) to observe the scintillations in GPS signal. Unfortunately, the experiment needs a constant GPS lock to achieve tangible results and due to the high orbit, this is hard to achieve using only one GPS antenna, as the pointing of the satellite is not adjusted for this experiment. However, GPS lock was achieved during the mission and the results were compared to TLE predictions, where an absolute position error of 5 km was calculated when 6 satellites were used for the lock. On the other hand, the NANOhpm-obc is to this date operating nominally, which confirms the robustness of the system.

3 SCIENTIFIC RESULTS

After successful commissioning of the satellite, the spacecraft operations were fully automated, including ground segment scheduling, satellites housekeeping procedures, mode selection according to available power and data acquisition for the experiments, thus employing a true remote sensing application like terrestrial IoT. Until now, more than 100k log entries were recorded on the ground segment.

3.1 Radiation experiments

The TRISAT-R mission encapsulated the radiation experiments inside the radiation shield, therefore the occurrence of SEEs was limited. Consequentially, higher emphasis was put to TID readings. For a better evaluation of the results, the TID was simulated for TID experiments using the FASTRAD tool, with both Ray-Tracing (RT) and Reverse Monte Carlo (RMC) techniques based on the detailed CAD model of the satellite. The predicted TID for 2 years per sensor positions are presented in Table I and are compatible with the initial SHIELDOSE-2 prediction, as the values for TID in the detailed 3D model fall in-between the solid-sphere and finite slab predictions.

Table I. Predicted TID values for 2 years per sensor position.

Target	TID – RT [krad]	TID – RMC [krad]
TID Monitor	4.7	2.5
FGDOS	5.1	2.9
SpaceRadMon	5.5	2.7

The gathered data from CHIMERA is analysed by ESA, and confirms the nominal operation of the experiment. CHIMERA is designed to detect SEE and the expected SEE rate inside the thick TRISAT-R Aluminium shielding is low, still a few SBUs and a possible latch-up were detected. Due to the limited statistics, the focus of the in-flight data analysis was aimed at the TID experiments.
The results from TID monitor were analysed by University of Maribor with support from SkyLabs. Figure 5 presents the accumulated dose during 1 month of observation, during which the experiment was actively monitoring the radiation for 7.35 days and accumulated 44.6 rad. Based on such rate, the yearly dose is estimated as 2.21 krad/year, which aligns with the simulated dose range of 1.25-2.35 krad/year from Table I. As the TID is measured only when the experiment is active, we relied on passive TID experiments for mission TID analysis.

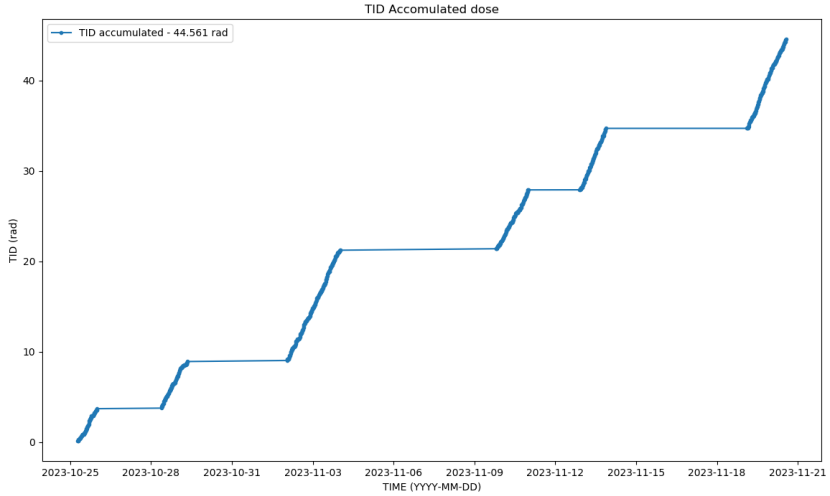

Figure 5. Accumulated radiation dose of TID monitor for 1 month of observations.

The TID data for FGDOS and SpaceRadMon were analysed by CERN and are presented on Figure 6. During the observation period, the total accumulated dose is approximately 2.5 krad for 14 months of analysed data. The accumulated dose from FGDOS and SpaceRadMon is also within the simulated values.

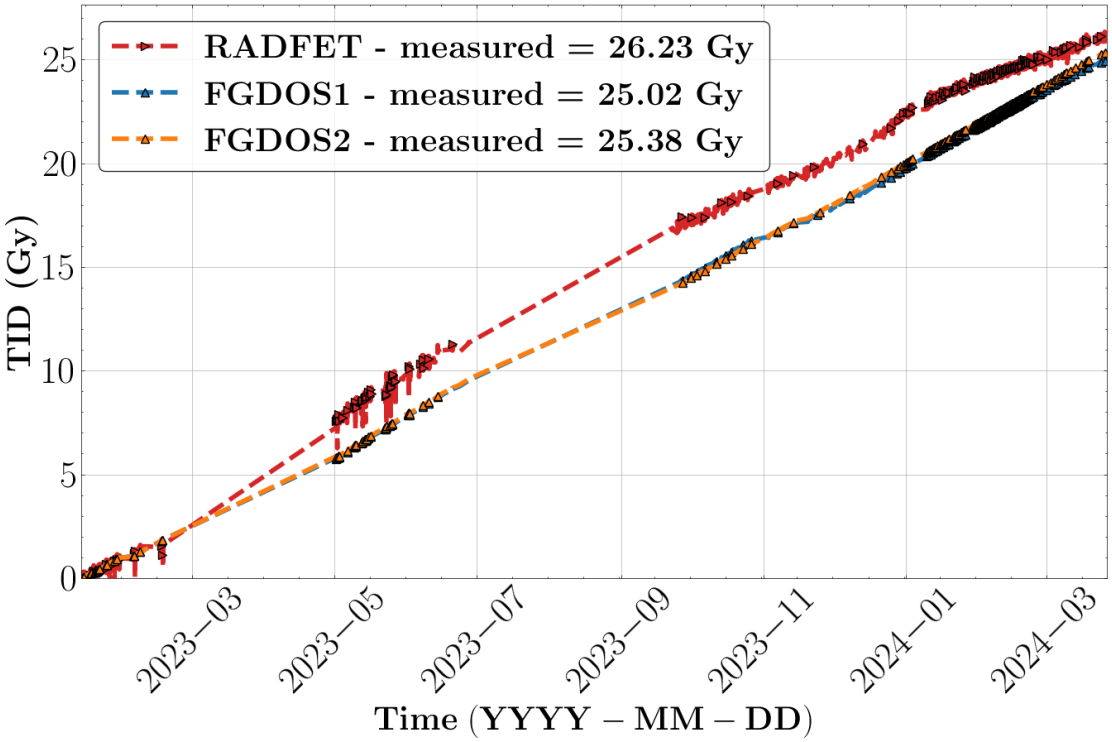

Figure 6. TID measurements for FGDOS and SpaceRadMon RADFET.

3.2 Camera modules

The camera modules are next to solar panels the only electronic circuits outside of the Aluminium shield and are operating nominally to this date. During the mission several occurrences of the black sun effect were measured, as can be seen on Figure 7 (left). The effect is observable as the black dot in the bottom left corner of the image. Due to the missing BGA underfill for camera, the reflection from PCB results in trace artifacts during high illuminance, which can also be seen on the image as black squares. We managed to utilise the cameras to capture an image from the Earth and to the best of our knowledge this a first picture of the Earth from MEO orbit performed by a 3U satellite. On Figure 8 a by factor of two upscaled image with extracted colours from Bayer pattern can be seen.

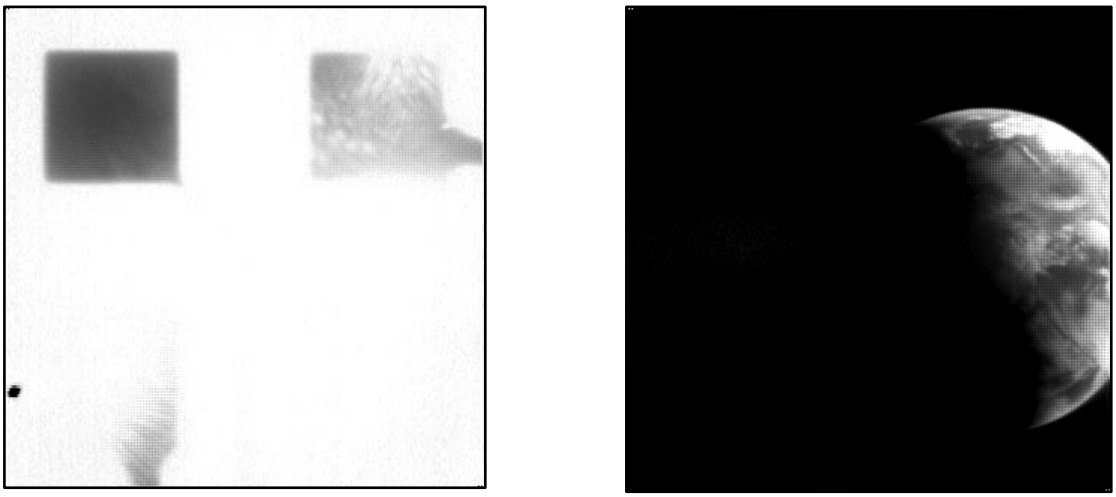

Figure 7. Black Sun effect (left) and raw capture of the Earth (right).

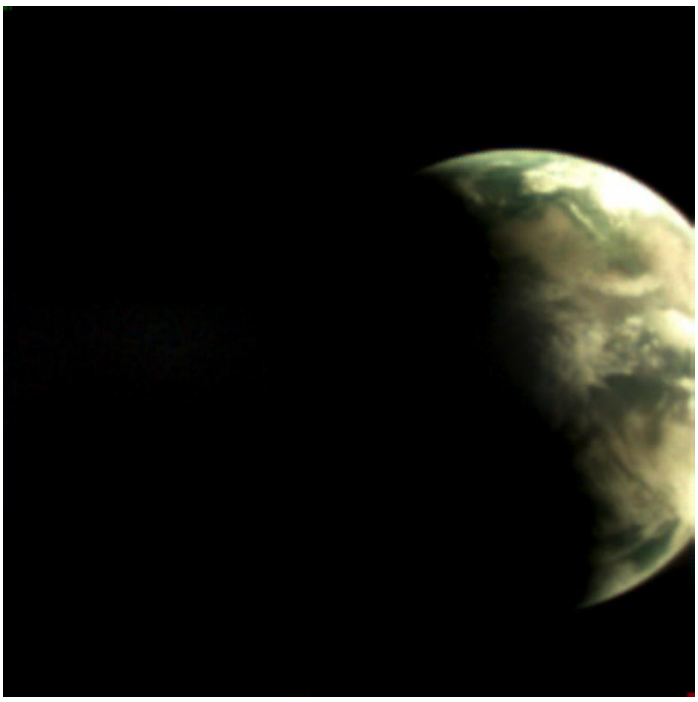

Figure 8. Earth through a 2-mm lens - technology image of the week by ESA [18].

4 CONCLUSION

TRISAT-R proved to be a robust nanosatellite in a very challenging orbit. Up to this date no critical radiation-based anomaly was observed, and, thanks to the shielding strategy, also no component degradation was observed, with exception of the solar panels, which are expectedly slowly losing maximum power capabilities due to their exposure to a high radiation environment. As it seems, the solar panel degradation will determine the end of life for TRISAT-R, but according to current predictions, we anticipate at least one more year of operation. The avionics platform FDIR mechanism also performed nominally, and during the mission we were able to perform two full firmware upgrades and 3 patches. The presented mission showed the potential as self-sufficient 3U remote sensing probes in MEO orbit, paving the way for a next generations of power optimized sensing probes for multi-point data collection. The on-board radiation monitoring experiments also performed well, and further development is anticipated in accordance with mission results.

5 ACKNOWLEDGEMENT

This work was supported by the Slovenian Research Agency under Grant P2-0069.
The TRISAT-R mission was partially financed by ESA and Slovenian company SkyLabs.

6 REFERENCES

[1] E. Kulu, “Nanosatellite Launch Forecasts - Track Record and Latest Prediction,” *Small Satellite Conference*, Aug. 2022, [Online]. Available: https://digitalcommons.usu.edu/smallsat/2022/all2022/7

[2] “Nanosats Database | Constellations, companies, technologies and more.” Accessed: Apr. 10, 2024. [Online]. Available: https://www.nanosats.eu/#figures

[3] F. Perez *et al.*, “DustCube, a nanosatellite mission to binary asteroid 65803 Didymos as part of the ESA AIM mission,” *Advances in Space Research*, vol. 62, no. 12, pp. 3335–3356, Dec. 2018, doi: 10.1016/j.asr.2018.06.019.
[4] T. Zushi *et al.*, “Small sensor probe for measuring plasma waves in space,” *Earth Planet Sp*, vol. 67, no. 1, p. 127, Aug. 2015, doi: 10.1186/s40623-015-0298-8.
[5] S. A. Bendoukha, K. Okuyama, S. Bianca, and M. Nishio, “Control System Design of an Ultra-small Deep Space Probe,” *Energy Procedia*, vol. 100, pp. 537–550, Nov. 2016, doi: 10.1016/j.egypro.2016.10.216.
[6] I. F. Akyildiz and A. Kak, “The Internet of Space Things/CubeSats,” *IEEE Network*, vol. 33, no. 5, pp. 212–218, Sep. 2019, doi: 10.1109/MNET.2019.1800445.
[7] A. Kak and I. F. Akyildiz, “Designing Large-Scale Constellations for the Internet of Space Things With CubeSats,” *IEEE Internet of Things Journal*, vol. 8, no. 3, pp. 1749–1768, Feb. 2021, doi: 10.1109/JIOT.2020.3016889.
[8] I. Priyadarshini, B. Bhola, R. Kumar, and C. So-In, “A Novel Cloud Architecture for Internet of Space Things (IoST),” *IEEE Access*, vol. 10, pp. 15118–15134, 2022, doi: 10.1109/ACCESS.2022.3144137.
[9] “SPENVIS - Space Environment, Effects, and Education System.” Accessed: Apr. 03, 2024. [Online]. Available: https://www.spenvis.oma.be/
[10] D. Selcan, G. Kirbis, and I. Kramberger, “Analog maximum power point tracking for spacecraft within a low earth orbit,” *IEEE Transactions on Aerospace and Electronic Systems*, vol. 52, no. 1, pp. 368–378, Feb. 2016, doi: 10.1109/TAES.2015.140279.
[11] D. Selčan, G. Kirbiš, and I. Kramberger, “Nanosatellites in LEO and Beyond: Advanced Radiation Protection Techniques for COTS-based Spacecraft,” *Acta Astronautica*, vol. 131, Nov. 2016, doi: 10.1016/j.actaastro.2016.11.032.
[12] L. Gonzales, D. Selčan, G. Kirbiš, and I. Kramberger, “FAULT TOLERANT TID MONITOR MODULE WITH SERIAL INTERFACE,” in *Proceedings of the 4S Symposium 2018*, 2018.
[13] “ESA - CHIMERA Board.” Accessed: Apr. 11, 2024. [Online]. Available: https://www.esa.int/Enabling_Support/Space_Engineering_Technology/Onboard_Computers_and_Data_Handling/CHIMERA_Board
[14] M. Álvarez, C. Hernando, J. Cesari, Á. Pineda, and E. García-Moreno, “Total Ionizing Dose Characterization of a Prototype Floating Gate MOSFET Dosimeter for Space Applications,” *IEEE Transactions on Nuclear Science*, vol. 60, no. 6, pp. 4281–4288, Dec. 2013, doi: 10.1109/TNS.2013.2288573.
[15] J. Dijks, “Precise LEO space radiation monitoring using the Space RadMon-NG payload,” 2023, Accessed: Apr. 11, 2024. [Online]. Available: https://repository.tudelft.nl/islandora/object/uuid%3A70bdbfdc-28be-40b5-864e-92798b910449
[16] A. Coronetti *et al.*, “The CELESTA CubeSat In-Flight Radiation Measurements and their Comparison with Ground Facilities Predictions,” *IEEE Transactions on Nuclear Science*, pp. 1–1, 2024, doi: 10.1109/TNS.2024.3376749.
[17] H.-J. Kim, “A Sun-Tracking CMOS Image Sensor With Black-Sun Readout Scheme,” *IEEE Transactions on Electron Devices*, vol. 68, no. 3, pp. 1115–1120, Mar. 2021, doi: 10.1109/TED.2021.3052450.
[18] “ESA - Earth through a 2-mm lens.” Accessed: Apr. 12, 2024. [Online]. Available: https://www.esa.int/ESA_Multimedia/Images/2023/11/Earth_through_a_2-mm_lens